

Enantioselective Iridium-Catalyzed Allylation of Nitroalkanes: Entry to β -Stereogenic α -Quaternary Primary Amines

Woo-Ok Jung, Binh Khanh Mai, Brian J. Spinello, Zachary J. Dubey, Seung Wook Kim, Craig E. Stivala,* Jason R. Zbieg,* Peng Liu,* and Michael J. Krische*



Cite This: *J. Am. Chem. Soc.* 2021, 143, 9343–9349



Read Online

ACCESS |

Metrics & More

Article Recommendations

Supporting Information

ABSTRACT: The first systematic study of simple nitronate nucleophiles in iridium-catalyzed allylic alkylation is described. Using a tol-BINAP-modified π -allyliridium C,O-benzoate catalyst, α,α -disubstituted nitronates substitute racemic branched alkyl-substituted allylic acetates, thus providing entry to β -stereogenic α -quaternary primary amines. DFT calculations reveal early transition states that render the reaction less sensitive to steric effects and distinct trans-effects of diastereomeric chiral-at-iridium π -allyl complexes that facilitate formation of congested tertiary–quaternary C–C bonds.

Chiral amines are prevalent among FDA-approved drugs,¹ as are protocols for their synthesis.² The vast majority of catalytic enantioselective methods for the construction of chiral amines deliver N-substituted carbon stereocenters.² Catalytic enantioselective methods applicable to the formation of acyclic chiral β -stereogenic amines are far less common and encompass asymmetric hydrogenation of enamines,³ allylic amines/amides⁴ or nitroolefins,⁵ 1,4-reductions and 1,4-additions to nitroolefins,^{6,7} and dynamic kinetic resolutions via aldehyde reductive amination.⁸ These methods do not deliver chiral β -stereogenic α -quaternary primary amines. Catalytic enantioselective Tsuji–Trost nitronate allylic alkylation–reduction potentially provides access to acyclic chiral β -stereogenic amines, but such methods are underdeveloped.^{9–12} Palladium-catalyzed allylic alkylations typically display linear regioselectivity and consequently focus on reactions that proceed via symmetric π -allylpalladium intermediates⁹ or prochiral nucleophiles (α -nitroesters).¹² Beyond vinyl epoxides,^{10a} only a single system for catalytic asymmetric allylic alkylation of unactivated nitronates with monosubstituted π -allyl precursors that displays branched regioselectivity has been described.^{10b,c} Only two examples of corresponding iridium-catalyzed nitronate allylic alkylations are reported.¹¹ Both the palladium- and iridium-based catalyst systems rely on linear aryl-substituted π -allyl precursors and display incomplete diastereo- and regioselectivity (Figure 1).

In connection with studies of π -allyliridium C,O-benzoate-catalyzed *nucleophilic* allylations of carbonyl compounds,¹³ we recently found these same complexes are competent catalysts for *electrophilic* allylation, as demonstrated in regio- and enantioselective aminations of racemic branched alkyl-substituted allylic acetates to form acyclic chiral α -stereogenic amines.¹⁴ Aspiring to access corresponding chiral β -stereogenic amines, a study of nitronate nucleophiles was undertaken. Here, we demonstrate that α,α -disubstituted nitroalkanes participate in highly enantioselective allylic alkylation with racemic branched alkyl-substituted allylic acetates. Despite forming congested contiguous quaternary–tertiary C–C

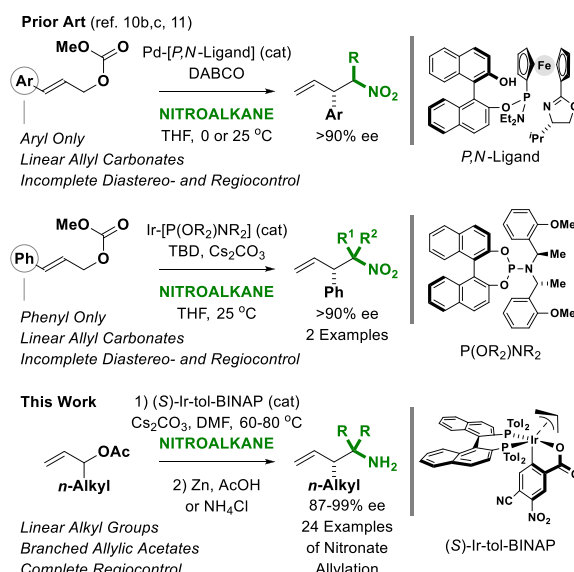


Figure 1. Unactivated nitronates in catalytic enantioselective allylic alkylations of monosubstituted π -allyl precursors.

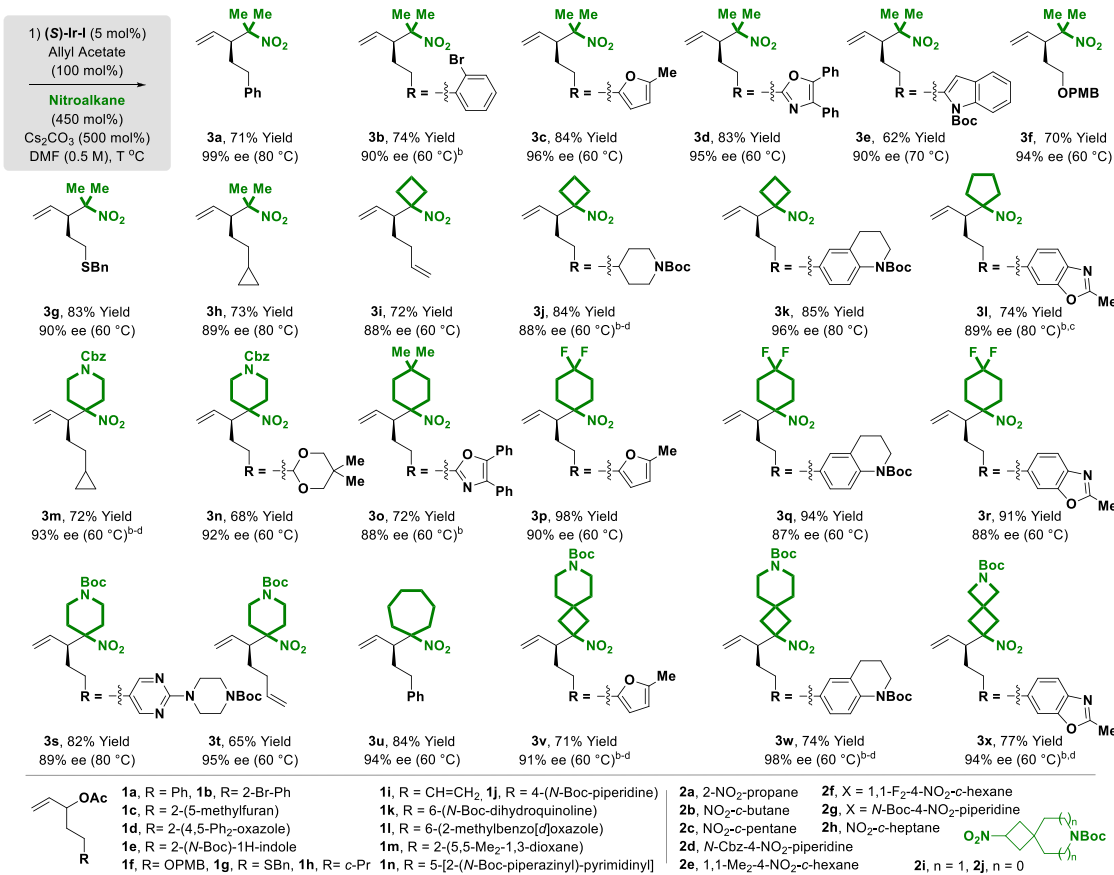
bonds, complete branched regioselectivities are observed. DFT calculations reveal early transition states that render the reaction less sensitive to steric effects and distinct trans-effects of diastereomeric chiral-at-iridium π -allyl complexes that facilitate formation of congested tertiary–quaternary C–C bonds.

Received: May 20, 2021

Published: June 21, 2021



Scheme 1. Iridium-Catalyzed Allylation of Nitroalkanes 2a–2j Using Allylic Acetates 1a–1n to Form Homoallylic Nitroalkanes 3a–3x^a



^aYields are of material isolated by silica gel chromatography. Enantioselectivities were determined by chiral stationary phase HPLC analysis. ^bNMP was used as the reaction solvent. ^c(S)-Ir-tol-BINAP, X = OMe. ^dIr-catalyst (10 mol%). See the Supporting Information for experimental details.

In initial experiments, allylic acetate 1a (100 mol%) was exposed to 2-nitropropane 2a (1125 mol%) as solvent (1.0 M) in the presence of Cs₂CO₃ (500 mol%) and the π -allyliridium C,O-benzoate complex modified by (S)-tol-BINAP, Ir-I, at 100 °C. The homoallylic nitroalkane 3a was formed in 51% yield and 95% ee (Table 1, entry 1). Lower loading of 2-nitropropane 2a (450 mol%) with DMF (0.5 M) as solvent improved yield and enantioselectivity (Table 1, entry 2), but further reduction in the loading of 2a led to a small decrease in yield (Table 1, entry 3). A slight decrease in temperature (80 °C) improved the yield of 3a without diminishing enantioselectivity (Table 1, entry 4). Lower loading of Cs₂CO₃ decreased the yield of 3a (Table 1, entry 5), and water (100 mol%) dramatically decreased conversion of 1a (Table 1, entry 6). Other π -allyliridium C,O-benzoates were evaluated but did not improve the yield of 3a (Table 1, entries 7–10).

To evaluate reaction scope, optimal conditions for the formation of 3a (Table 1, entry 4) were applied to the allylic alkylation of α,α -disubstituted nitroalkanes 2a–2j with racemic branched alkyl-substituted allylic acetates 1a–1n (Scheme 1). As illustrated by the conversion of 2-nitropropane 2a to adducts 3a–3h, diverse (hetero)aromatic groups (3a–3e), (thio)ethers (3f and 3g), and cyclopropyl groups (3h) are tolerated. As demonstrated by the formation of adducts 3i–3x, cyclic nitroalkanes 2b–2h are also competent partners for allylic alkylation. This includes nitrocyclobutane (2b), nitrocyclopentane (2c), N-Cbz- and N-Boc-4-nitropiperidines (2d

Table 1. Selected Optimization Experiments in the Enantioselective Ir-Catalyzed Allylic Alkylation of Racemic Branched Alkyl-Substituted Allylic Acetate 1a with Nitronate 2a^a

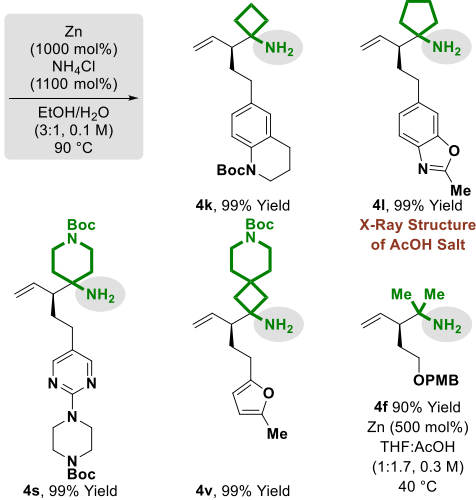
Entry	2a (mol%)	catalyst	Cs ₂ CO ₃ (mol%)	T °C	Yield (%)	ee (%)
1 ^b	1125	Ir-I	500 mol%	100	51	95
2	450	Ir-I	500 mol%	100	67	99
3	240	Ir-I	500 mol%	100	35	99
4	450	Ir-I	500 mol%	80	71	99
5	450	Ir-I	300 mol%	80	56	99
6 ^c	450	Ir-I	500 mol%	80	<10	-
7	450	Ir-II	500 mol%	80	51	99
8	450	Ir-III	500 mol%	80	53	99
9	450	Ir-IV	500 mol%	80	43	99
10	450	Ir-V	500 mol%	80	50	99

Ir-II: L = (S)-tol-BINAP, X = CN Ir-IV: L = (S)-SEPHOS, X = CN
 Ir-III: L = (S)-tol-BINAP, X = NO₂ Ir-V: L = (S)-MeO-BIPHEP, X = CN
 Ir-II: L = (S)-BINAP, X = CN

^aYields are of material isolated by silica gel chromatography. Enantioselectivities were determined by HPLC analysis. ^b2a = solvent (1.0 M). ^cH₂O (100 mol%). See the Supporting Information for experimental details.

and **2g**, respectively), as well as 1,1-disubstituted 4-nitrocyclohexanes (**2e** and **2f**), nitrocycloheptane (**2h**), and the spirocyclic nitroalkanes (**2i** and **2j**). In all cases, good to excellent yields of adducts **3a–3x** were obtained with high levels of enantiomeric enrichment (87–99% ee) and complete branched regioselectivity. The nonsymmetric nitroalkane (1-nitroethyl)benzene provided high yields of allylic alkylation product, but low diastereomeric ratios were observed. Low conversions were observed using allylic acetates bearing α - or β -branched alkyl moieties. As revealed by the conversion of **3f**, **3k**, **3l**, **3s**, and **3v** to amines **4f**, **4k**, **4l**, **4s** and **4v**, respectively, zinc-mediated reduction of the allylation products provides entry to chiral β -stereogenic α -quaternary primary amines (Scheme 2).

Scheme 2. Zinc-Mediated Reduction of **3f**, **3k**, **3l**, **3s**, and **3v** to Form β -Stereogenic α -Quaternary Primary Amines **4f**, **4k**, **4l**, **4s**, and **4v**^a



^aYields are of material isolated after filtration through Celite. See the Supporting Information for experimental details.

Density functional theory (DFT) calculations were carried out to investigate the origin of regio- and enantioselectivity of the Ir-catalyzed allylic alkylation.^{15,16} As numerous diastereomeric π -allyliridium C_2O -benzoate complexes may exist in equilibrium prior to the allylation, the relative stabilities, reactivities, and regioselectivities of all 16 possible stereoisomers of the π -crotyliridium(III) complex were computed (Figure 2). These include diastereomers **A**, **B**, **C**, and **D**, where the C_2O -benzoate resides in different coordination sites of the octahedral Ir complex,¹⁷ with four different coordination modes of the π -crotyl ligand for each diastereomer. Here, the suffix *exo* or *endo* describes whether the allyl C2–H points away or toward the C_2O -benzoate ligand, and *distal* or *proximal* describes if the C3–methyl points away or toward the C_2O -benzoate (see Figure S2 for the relative stabilities of all 16 isomers). Computed activation barriers for the addition of $^{17}\text{CMe}_2\text{NO}_2$ anion to each π -crotyliridium(III) isomer leading to branched and linear products are shown in Figure 2B. The 16 π -crotyliridium(III) isomers exhibited very different reactivity and regioselectivity. The most reactive isomer, **D_exo_proximal**, strongly favors the branched product ($\Delta\Delta G^\ddagger(B-L) = -8.5$ kcal/mol), while some less reactive isomers, such as **A_endo_proximal** and **B_endo_proximal**,

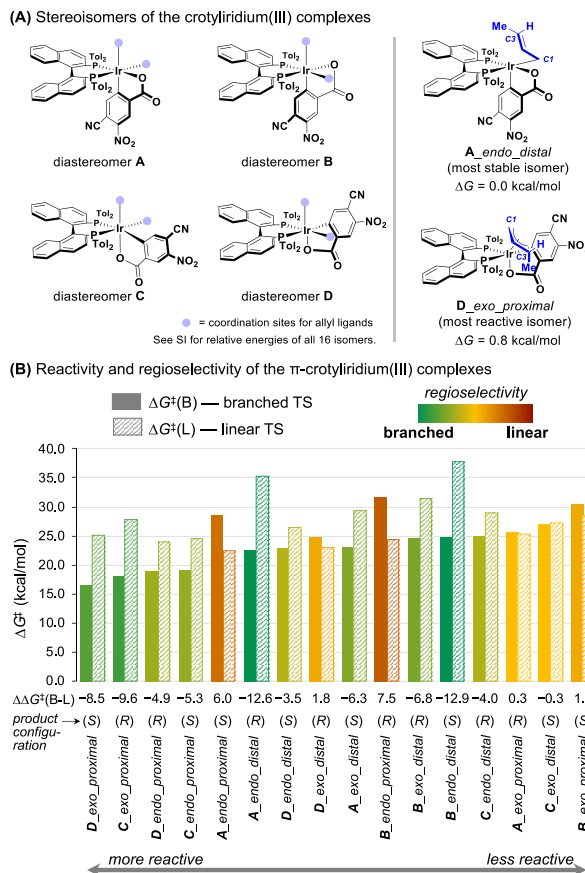


Figure 2. Computed activation free energies of the addition of $^{17}\text{CMe}_2\text{NO}_2$ to different π -crotyliridium(III) isomers. All activation barriers (ΔG^\ddagger) are with respect to **A_endo_distal**.

prefer the linear product. These results suggest stereogenicity at iridium affects not only reactivity but also regioselectivity. To assess the origin of these effects, computational analyses on the electronic and structural properties of the diastereomeric π -crotyliridium(III) complexes were performed.

The computed transition-state structures of the outer sphere addition of the nitronate nucleophile all involve long forming C–C distances (usually >2.4 Å in branch-selective TSs and >2.2 Å in linear-selective TSs (see Figure 3 and Figure S4 in the Supporting Information)). These early transition states suggest that the addition is not sensitive to steric effects, and thus, the regioselectivity is mainly controlled by the electronic properties of the π -allyl complexes. The computed ground-state properties of the π -crotyliridium(III) isomers and the distortion/interaction model analysis of the allylation transition states revealed enormously different electronic properties and their influences on the regioselectivity. In branch-selective isomers, such as **D_exo_proximal** (Figure 3A), the Ir–C3 distance is much longer than Ir–C1. This geometry leads to weaker d $\rightarrow\pi^*$ backbonding at C3 and more positive charge on C3 compared to C1 (Figure 3A),¹⁸ making the more substituted C3 terminus more electrophilic.¹⁹ In addition, the transition state of nitronate addition to C3 (TS-1) is promoted by the smaller distortion energy of the π -crotyliridium complex ($\Delta E_{\text{dist-Ir}}$) as the ground-state Ir–C3 bond of **D_exo_proximal** is predistorted to a longer distance (2.50 Å) that is closer to that in TS-1 (2.87 Å). In contrast, electronic effects strongly disfavor branch-selective addition with

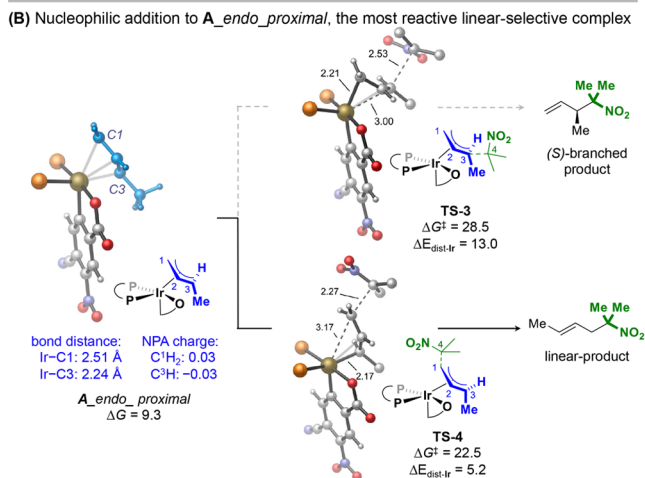
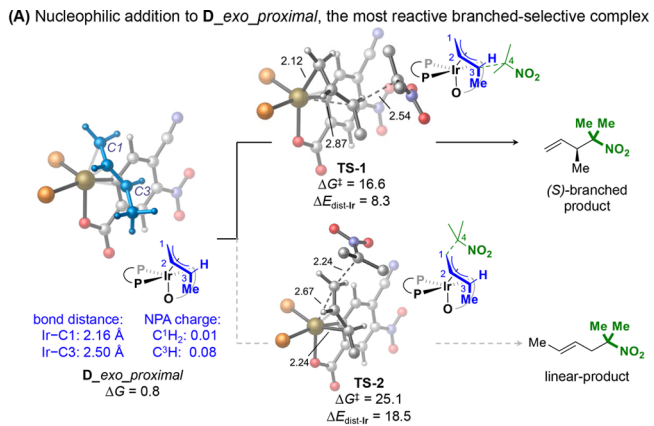
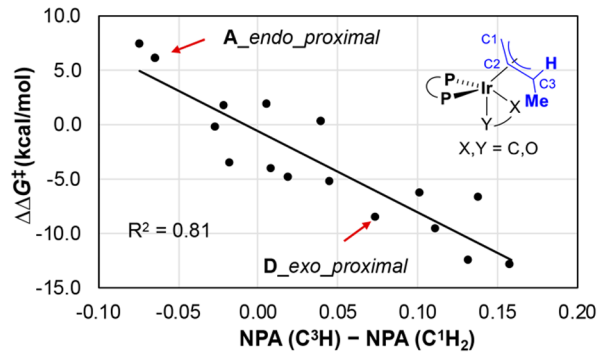


Figure 3. Origin of regioselectivity. Bisphosphine ligand and some H atoms are omitted for clarity. All Gibbs free energies are in kcal/mol with respect to **A_endo_distal**. $\Delta E_{\text{dist}-\text{Ir}}$: distortion energy of the π -crotyliridium complex to reach its geometry in the TS for nucleophilic addition.

A_endo_proximal (Figure 2B), because the more substituted terminus C3 is less electrophilic than C1, as evidenced by the negative charge on C3. In addition, the Ir–C3 bond becomes shorter than Ir–C1, leading to greater distortion energy ($\Delta E_{\text{dist}-\text{Ir}}$) to elongate the Ir–C3 bond in the branch-selective transition state (TS-3).

The same analyses on all 16 isomers of the π -crotyliridium complex revealed good correlations between the computed regioselectivity for each isomer and the C3/C1 difference in NPA charge and Ir–C3 bond distance; that is, diastereomers with more positive charge on C3 and a longer Ir–C3 bond give higher branch-selectivity (Figure 4).²⁰ These results are consistent with our findings that regioselectivity is controlled by electronic effects, including the allyl electrophilicity and the distortion of the π -allyl complex. The electronic properties of the diastereomeric π -crotyl complexes also are affected by the trans-effect²¹ of the bisphosphine and the chelating C,O-benzoate ligands on the stereogenic Ir center. In diastereomers A and B, because of the stronger trans-effect of the aryl versus phosphine groups, addition occurs at sites *trans* to the aryl group, leading to branched products in “distal” isomers and linear products in “proximal” isomers. In diastereomers C and D, “proximal” isomers, in which C3 is *trans* to a phosphorus atom, give higher branched regioselectivity. This is consistent with the stronger trans-effects of phosphine versus carboxylate

(A) Correlation between NPA charge difference between allyl termini and computed regioselectivity



(B) Correlation between Ir–C3 distance and computed regioselectivity

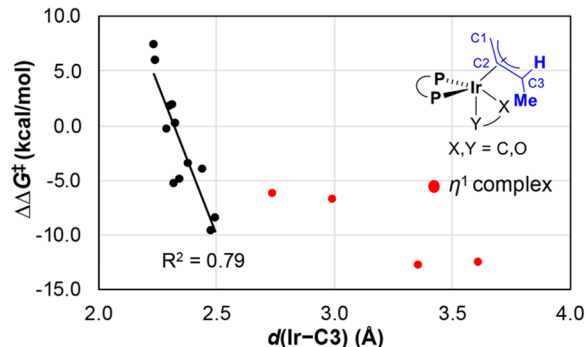


Figure 4. Electronic effects on allylation regioselectivity of different stereoisomers of the π -crotyliridium complex.

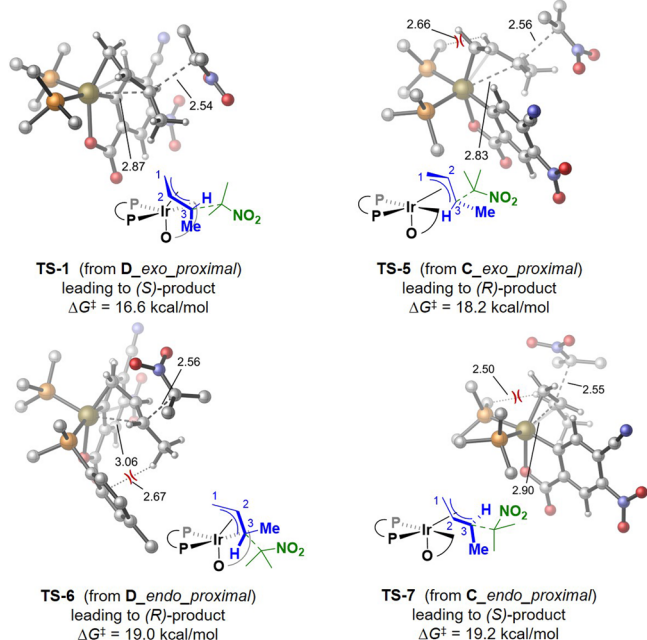


Figure 5. Optimized structures for additions of ${}^-\text{CMe}_2\text{NO}_2$ anion giving branched product. Gibbs free energies are with respect to **A_endo_distal**.

ligands. These branch-selective “proximal” isomers of C and D are also among the most reactive in all 16 stereoisomers (Figure 2B), as the π -acceptor ability of the phosphine ligand promotes addition at sites *trans* to phosphorus.²²

Stereogenicity at iridium is also a critical determinant of enantioselectivity. Because of trans-effects (*vide supra*), the “*proximal*” isomers of C and D are the most reactive among all 16 stereoisomers. The four most favorable pathways involve **D_{exo}-proximal (TS-1)** and **C_{endo}-proximal (TS-7)**, which give (S)-product, and **D_{endo}-proximal (TS-6)** and **C_{exo}-proximal (TS-5)**, which give (R)-product. Optimized structures of these branch-selective transition states are shown in Figure 5. The two transition states leading to the (R)-product, TS-5 and TS-6, are destabilized because the allyl C2–H moiety in TS-5 and the C3–methyl in TS-6 clash with a *P*-tolyl group of (S)-tol-BINAP. Thus, TS-5 and TS-6 are 1.6 and 1.8 kcal/mol less stable than the lowest-energy transition state, TS-1, that gives the (S)-product. In TS-1, the steric repulsions between tol-BINAP and the allyl group are absent. Our calculations are consistent with the experimentally observed enantioselectivity for the (S)-product.

In summary, we report iridium-catalyzed allylic alkylations of nitronate nucleophiles. This method, which employs an air- and water-stable π -allyliridium *C,O*-benzoate catalyst modified by tol-BINAP, enables highly regio- and enantioselective substitution of racemic branched alkyl-substituted allylic acetates by α,α -disubstituted nitronates and, hence, entry to β -stereogenic α -quaternary primary amines. As revealed by DFT calculations, early transition states that render the reaction less sensitive to steric effects and distinct trans-effects of diastereomeric chiral-at-iridium π -allyl complexes facilitate formation of congested tertiary–quaternary C–C bonds. Related asymmetric allylic alkylations of nonstabilized carbanions are currently underway.²³

■ ASSOCIATED CONTENT

SI Supporting Information

The Supporting Information is available free of charge at <https://pubs.acs.org/doi/10.1021/jacs.1c05212>.

Experimental procedures; spectroscopic and chromatographic data for all new compounds (^1H NMR, ^{13}C NMR, IR, and HRMS), including HPLC traces for racemic and enantiomerically enriched compounds; computational details; single-crystal X-ray diffraction data for compound 4l (PDF)

Accession Codes

CCDC 2081056 contains the supplementary crystallographic data for this paper. These data can be obtained free of charge via www.ccdc.cam.ac.uk/data_request/cif, or by emailing data_request@ccdc.cam.ac.uk, or by contacting The Cambridge Crystallographic Data Centre, 12 Union Road, Cambridge CB2 1EZ, UK; fax: +44 1223 336033.

■ AUTHOR INFORMATION

Corresponding Authors

Craig E. Stivala — *Discovery Chemistry, Genentech, Inc., South San Francisco, California 94080, United States;*
ORCID.org/0000-0002-5024-6346; Email: stivala.craig@gene.com

Jason R. Zbieg — *Discovery Chemistry, Genentech, Inc., South San Francisco, California 94080, United States;*
ORCID.org/0000-0002-2897-8911; Email: zbieg.jason@gene.com

Peng Liu — *Department of Chemistry, University of Pittsburgh, Pittsburgh, Pennsylvania 15260, United States;* ORCID.org/0000-0002-8188-632X; Email: pengliu@pitt.edu

Michael J. Krische — *Department of Chemistry, University of Texas at Austin, Austin, Texas 78712, United States;*
ORCID.org/0000-0001-8418-9709; Email: mkrische@mail.utexas.edu

Authors

Woo-Ok Jung — *Department of Chemistry, University of Texas at Austin, Austin, Texas 78712, United States*

Binh Khanh Mai — *Department of Chemistry, University of Pittsburgh, Pittsburgh, Pennsylvania 15260, United States;*
ORCID.org/0000-0001-8487-1417

Brian J. Spinello — *Department of Chemistry, University of Texas at Austin, Austin, Texas 78712, United States*

Zachary J. Dubey — *Department of Chemistry, University of Texas at Austin, Austin, Texas 78712, United States*

Seung Wook Kim — *Department of Chemistry, University of Texas at Austin, Austin, Texas 78712, United States*

Complete contact information is available at:
<https://pubs.acs.org/10.1021/jacs.1c05212>

Notes

The authors declare no competing financial interest.

■ ACKNOWLEDGMENTS

The Robert A. Welch Foundation (F-0038) and the NIH-NIGMS (RO1-GM069445, 1 S10 OD021508-01, R35 GM128779) are acknowledged. We thank Mr. Weijia Shen and Ms. Sakiko Sumikura for skillful technical assistance. Genentech is acknowledged for summer predoctoral internship support (W.-O.J., B.J.S., and S.W.K.). DFT calculations were carried out at the Center for Research Computing at the University of Pittsburgh, the Extreme Science and Engineering Discovery Environment (XSEDE), and the TACC Frontera Supercomputer supported by the National Science Foundation Grant Number ACI-1548562. We thank Dr. Michael Ruf of Bruker AXS for acquisition of crystallographic data.

■ REFERENCES

- (1) It was estimated in 2014 that chiral amines constitute roughly 40% of new FDA-approved small-molecule drugs: Jarvis, L. M. *Chem. Eng. News* **2014**, 94, 12–17.
- (2) For selected reviews on the synthesis of chiral amines, see: (a) Enders, D.; Reinhold, U. *Asymmetric Synthesis of Amines by Nucleophilic 1,2-Addition of Organometallic Reagents to the CN-Double Bond*. *Tetrahedron: Asymmetry* **1997**, 8, 1895–1946. (b) Bloch, R. *Additions of Organometallic Reagents to C = N Bonds: Reactivity and Selectivity*. *Chem. Rev.* **1998**, 98, 1407–1438. (c) Robak, M. T.; Herbage, M. A.; Ellman, J. A. *Synthesis and Applications of tert-Butanesulfonamide*. *Chem. Rev.* **2010**, 110, 3600–3740. (d) *Chiral Amine Synthesis: Methods, Developments and Applications*; Nugent, T. C., Ed.; Wiley-VCH, 2010. (e) Nugent, T. C.; El-Shazly, M. *Chiral Amine Synthesis – Recent Developments and Trends for Enamide Reduction, Reductive Amination, and Imine Reduction*. *Adv. Synth. Catal.* **2010**, 352, 753–819. (f) *Stereoselective Formation of Amines*; Li, W., Zhang, X., Eds.; Topics in Current Chemistry; Springer, 2014; Vol. 343. (g) Mailyan, A. K.; Eickhoff, J. A.; Minakova, A. S.; Gu, Z.; Lu, P.; Zakarian, A. *Cutting-Edge and Time-Honored Strategies for Stereoselective Construction of C–N Bonds in Total Synthesis*. *Chem. Rev.* **2016**, 116, 4441–4557. (h) Abdine, R. A. A.; Hedouin, G.; Colobert, F.; Wencel-Delord, J. *Metal-Catalyzed Asymmetric Hydrogenation of C=N Bonds*. *ACS Catal.* **2021**, 11, 215–247.
- (3) For chiral β -stereogenic amines via catalytic enantioselective hydrogenation of enamines derivatives (including dehydro- β -amino acid derivatives), see: (a) Elaridi, J.; Thaqi, A.; Prosser, A.; Jackson,

W. R.; Robinson, A. J. An Enantioselective Synthesis of β^2 -Amino Acid Derivatives. *Tetrahedron: Asymmetry* **2005**, *16*, 1309–1319. (b) Remarchuk, T.; Babu, S.; Stults, J.; Zanotti-Gerosa, A.; Roseblade, S.; Yang, S.; Huang, P.; Sha, C.; Wang, Y. An Efficient Catalytic Asymmetric Synthesis of a β^2 -Amino Acid on Multikilogram Scale. *Org. Process Res. Dev.* **2014**, *18*, 135–141. (c) Saito, N.; Abdullah, I.; Hayashi, K.; Hamada, K.; Koyama, M.; Sato, Y. Enantioselective Synthesis of β -Amino Acid Derivatives via Nickel-Promoted Regioselective Carboxylation of Ynamides and Rhodium-Catalyzed Asymmetric Hydrogenation. *Org. Biomol. Chem.* **2016**, *14*, 10080–10089. (d) Han, C.; Savage, S.; Al-Sayah, M.; Yajima, H.; Remarchuk, T.; Reents, R.; Wirz, B.; Iding, H.; Bachmann, S.; Fantasia, S. M.; Scalone, M.; Hell, A.; Hidber, P.; Gosselin, F. Asymmetric Synthesis of Akt Kinase Inhibitor Ipatasertib. *Org. Lett.* **2017**, *19*, 4806–4809. (e) Zhang, J.; Liu, C.; Wang, X.; Chen, J.; Zhang, Z.; Zhang, W. Rhodium-Catalyzed Asymmetric Hydrogenation of β -Branched Enamides for the Synthesis of β -Stereogenic Amines. *Chem. Commun.* **2018**, *54*, 6024–6027.

(4) For chiral β -stereogenic amines via catalytic enantioselective hydrogenation of allylic amines or amides to form acyclic chiral β -stereogenic amines, see: (a) Fahrang, R.; Sinou, D. Asymmetric Reduction of Allylamines and their Derivatives with Rhodium Complexes. *Bull. Soc. Chim. Belg.* **1989**, *98*, 387–393. (b) Wang, C.-J.; Sun, X.; Zhang, X. Enantioselective Hydrogenation of Allylphthalimides: An Efficient Method for the Synthesis of β -Methyl Chiral Amines. *Angew. Chem., Int. Ed.* **2005**, *44*, 4933–4935. (c) Steinhuebel, D. P.; Krksa, S. W.; Alorati, A.; Baxter, J. M.; Belyk, K.; Bishop, B.; Palucki, M.; Sun, Y.; Davies, I. W. Asymmetric Hydrogenation of Protected Allylic Amines. *Org. Lett.* **2010**, *12*, 4201–4203. (d) Ma, S.; Grinberg, N.; Haddad, N.; Rodriguez, S.; Busacca, C. A.; Fandrick, K.; Lee, H.; Song, J. J.; Yee, N.; Krishnamurthy, D.; Senanayake, C. H.; Wang, J.; Trenck, J.; Mendonsa, S.; Claise, P. R.; Gilman, R. J.; Evers, T. H. *Org. Process Res. Dev.* **2013**, *17*, 806–810. (e) Cabre, A.; Verdaguer, X.; Riera, A. Enantioselective Synthesis of β -Methyl Amines via Iridium-Catalyzed Asymmetric Hydrogenation of *N*-Sulfonyl Allyl Amines. *Adv. Synth. Catal.* **2019**, *361*, 4196–4200.

(5) For chiral β -stereogenic amines via catalytic enantioselective hydrogenation of nitroolefins, see: (a) Li, S.; Huang, K.; Cao, B.; Zhang, J.; Wu, W.; Zhang, X. Highly Enantioselective Hydrogenation of β,β -Disubstituted Nitroalkanes. *Angew. Chem., Int. Ed.* **2012**, *51*, 8573–8576. (b) Li, S.; Huang, K.; Zhang, J.; Wu, W.; Zhang, X. Rh-Catalyzed Highly Enantioselective Hydrogenation of Nitroalkenes under Basic Conditions. *Chem. - Eur. J.* **2013**, *19*, 10840–10844. (c) Zhao, Q.; Li, S.; Huang, K.; Wang, R.; Zhang, X. A Novel Chiral Bisphosphine-Thiourea Ligand for Asymmetric Hydrogenation of β,β -Disubstituted Nitroalkenes. *Org. Lett.* **2013**, *15*, 4014–4017. (d) Liu, M.; Kong, D.; Li, M.; Zi, G.; Hou, G. Iridium-Catalyzed Enantioselective Hydrogenation of β,β -Disubstituted Nitroalkenes. *Adv. Synth. Catal.* **2015**, *357*, 3875–3879. (e) Li, S.; Xiao, T.; Li, D.; Zhang, X. First Iridium-Catalyzed Highly Enantioselective Hydrogenation of β -Nitrocrylates. *Org. Lett.* **2015**, *17*, 3782–3785. (f) Yu, Y.-B.; Cheng, L.; Li, Y.-P.; Fu, Y.; Zhu, S.-F.; Zhou, Q.-L. Enantioselective Iridium-Catalyzed Hydrogenation of β,β -Disubstituted Nitroalkenes. *Chem. Commun.* **2016**, *52*, 4812–4815.

(6) For chiral β -stereogenic amines via conjugate reduction of nitroolefins (selected examples), see: (a) Czekelius, C.; Carreira, E. M. Catalytic Enantioselective Conjugate Reduction of β,β -Disubstituted Nitroalkenes. *Angew. Chem., Int. Ed.* **2003**, *42*, 4793–4795. (b) Soltani, O.; Ariger, M. A.; Carreira, E. M. Transfer Hydrogenation in Water: Enantioselective, Catalytic Reduction of (*E*)- β,β -Disubstituted Nitroalkenes. *Org. Lett.* **2009**, *11*, 4196–4198. (c) Chen, L.-A.; Xu, W.; Huang, B.; Ma, J.; Wang, L.; Xi, J.; Harms, K.; Gong, L.; Meggers, E. Asymmetric Catalysis with an Inert Chiral-at-Metal Iridium Complex. *J. Am. Chem. Soc.* **2013**, *135*, 10598–10601. (d) Martinelli, E.; Vicini, A. C.; Mancinelli, M.; Mazzanti, A.; Zani, P.; Bernardi, L.; Fochi, M. Catalytic Highly Enantioselective Transfer Hydrogenation of β -Trifluoromethyl Nitroalkenes. An Easy and General Entry to Optically Active β -Trifluoromethyl Amines. *Chem.*

Commun. **2015**, *51*, 658–660. (e) Bertolotti, M.; Brenna, E.; Crotti, M.; Gatti, F. G.; Monti, D.; Parmeggiani, F.; Santangelo, S. Substrate Scope Evaluation of the Enantioselective Reduction of β -Alkyl- β -arylnitroalkenes by Old Yellow Enzymes 1–3 for Organic Synthesis Applications. *ChemCatChem* **2016**, *8*, 577–583. (f) Xu, W.; Arieno, M.; Löw, H.; Huang, K.; Xie, X.; Cruchter, T.; Ma, Q.; Xi, J.; Huang, B.; Wiest, O.; Gong, L.; Meggers, E. Metal-Templated Design: Enantioselective Hydrogen-Bond-Driven Catalysis Requiring Only Parts-per-Million Catalyst Loading. *J. Am. Chem. Soc.* **2016**, *138*, 8774–8780.

(7) For chiral β -stereogenic amines via conjugate addition to nitroolefins (selected examples), see: (a) Mampreian, D. M.; Hoveyda, A. H. Efficient Cu-Catalyzed Asymmetric Conjugate Additions of Alkylzinc Reagents to Aromatic and Aliphatic Acyclic Nitroalkenes. *Org. Lett.* **2004**, *6*, 2829–2832. (b) Herrera, R. P.; Sgarzani, V.; Bernardi, L.; Ricci, A. Catalytic Enantioselective Friedel–Crafts Alkylation of Indoles with Nitroalkenes by Using a Simple Thiourea Organocatalyst. *Angew. Chem., Int. Ed.* **2005**, *44*, 6576–6579. (c) Itoh, J.; Fuchibe, K.; Akiyama, T. Catalytic Enantioselective Friedel–Crafts Alkylation of Indoles with Nitroalkenes by Using a Simple Thiourea Organocatalyst. *Angew. Chem., Int. Ed.* **2008**, *47*, 4016–4018. (d) Sheng, Y.-F.; Li, G.-Q.; Kang, Q.; Zhang, A.-J.; You, S.-L. Asymmetric Friedel–Crafts Reaction of 4,7-Dihydroindoles with Nitroolefins by Chiral Brønsted Acids under Low Catalyst Loading. *Chem. - Eur. J.* **2009**, *15*, 3351–3354. (e) Nishimura, T.; Sawano, T.; Tokaji, S.; Hayashi, T. Rhodium-Catalyzed Asymmetric Conjugate Alkylation of Nitroalkenes. *Chem. Commun.* **2010**, *46*, 6837–6839. (f) Arai, T.; Tsuchida, A.; Miyazaki, T.; Awata, A. Catalytic Asymmetric Synthesis of Chiral 2-Vinyldole Scaffolds by Friedel–Crafts Reaction. *Org. Lett.* **2017**, *19*, 758–761.

(8) For chiral β -stereogenic amines via dynamic kinetic asymmetric reductive amination, see: (a) Hoffmann, S.; Nicoletti, M.; List, B. Catalytic Asymmetric Reductive Amination of Aldehydes via Dynamic Kinetic Resolution. *J. Am. Chem. Soc.* **2006**, *128*, 13074–13075. (b) Fuchs, C. S.; Hollauf, M.; Meissner, M.; Simon, R. C.; Besset, T.; Reek, J. N. H.; Riethorst, W.; Zepeck, F.; Kroutil, W. Dynamic Kinetic Resolution of 2-Phenylpropanal Derivatives to Yield β -Chiral Primary Amines via Bioamination. *Adv. Synth. Catal.* **2014**, *356*, 2257–2265. (c) Villa-Marcos, B.; Xiao, J. Metal and Organo-Catalysed Asymmetric Hydroaminomethylation of Styrenes. *Chin. J. Catal.* **2015**, *36*, 106–112. (d) Meng, J.; Li, X.-H.; Han, Z.-Y. Enantioselective Hydroaminomethylation of Olefins Enabled by Rh/Bronsted Acid Relay Catalysis. *Org. Lett.* **2017**, *19*, 1076–1079. (e) Matzel, P.; Wenske, S.; Merdivan, S.; Günther, S.; Höhne, M. Synthesis of β -Chiral Amines by Dynamic Kinetic Resolution of α -Branched Aldehydes Applying Imine Reductases. *ChemCatChem* **2019**, *11*, 4281–4285.

(9) For use of unactivated nitronate nucleophiles in enantioselective palladium-catalyzed allylic alkylations that proceed by way of symmetric π -allylpalladium intermediates or display linear regioselectivity, see: (a) Rieck, H.; Helmchen, G. Palladium Complex Catalyzed Asymmetric Allylic Substitutions with Nitromethane: Enantioselectivities Exceeding 99.9% ee. *Angew. Chem., Int. Ed. Engl.* **1996**, *34*, 2687–2689. (b) Trost, B. M.; Surivet, J.-P. Diastereo- and Enantioselective Allylation of Substituted Nitroalkanes. *J. Am. Chem. Soc.* **2000**, *122*, 6291–6292. (c) Trost, B. M.; Surivet, J.-P. Asymmetric Allylic Alkylation of Nitroalkanes. *Angew. Chem., Int. Ed.* **2000**, *39*, 3122–3124. (d) Uozumi, Y.; Suzuka, T. π -Allylic C1-Substitution in Water with Nitromethane Using Amphiphilic Resin-Supported Palladium Complexes. *J. Org. Chem.* **2006**, *71*, 8644–864. (e) Maki, K.; Kanai, M.; Shibasaki, M. Pd-Catalyzed Allylic Alkylation of Secondary Nitroalkanes. *Tetrahedron* **2007**, *63*, 4250–4257.

(10) Isolated examples of the use of nitronate nucleophiles in enantioselective palladium-catalyzed allylic alkylation exist, but incomplete regioselectivities are typically observed: (a) Trost, B. M.; Jiang, C. Atom Economic Asymmetric Creation of Quaternary Carbon: Regio- and Enantioselective Reactions of a Vinyl epoxide with a Carbon Nucleophile. *J. Am. Chem. Soc.* **2001**, *123*, 12907–12908. (b) Yang, X.-F.; Ding, C.-H.; Li, X.-H.; Huang, J.-Q.; Hou, X.-L.; Dai,

L.-X.; Wang, P.-J. Regio- and Enantioselective Palladium-Catalyzed Allylic Alkylation of Nitromethane with Monosubstituted Allyl Substrates: Synthesis of (*R*)-Rolipram and (*R*)-Baclofen. *J. Org. Chem.* **2012**, *77*, 8980–8985. (c) Yang, X.-F.; Yu, W.-H.; Ding, C.-H.; Wan, S.-H.; Hou, X.-L.; Dai, L.-X.; Wang, P.-J. Palladium-Catalyzed Regio-, Diastereo-, and Enantioselective Allylation of Nitroalkanes with Monosubstituted Allylic Substrates. *J. Org. Chem.* **2013**, *78*, 6503–6509. (d) Yang, X.-F.; Li, X.-H.; Ding, C.-H.; Xu, C.-F.; Dai, L.-X.; Hou, X.-L. Pd-Catalyzed Allylic Alkylation of Dienyl Carbonates with Nitromethane with High C-5 Regioselectivity. *Chem. Commun.* **2014**, *50*, 484–486.

(11) Only one prior study of enantioselective iridium-catalyzed allylic alkylation of nitronate nucleophiles is reported, which mainly focused on reactions of α -nitroesters: Dahnz, A.; Helmchen, G. Iridium-Catalyzed Enantioselective Allylic Substitutions with Aliphatic Nitro Compounds as Prenucleophiles. *Synlett* **2006**, 0697–0700.

(12) For examples of enantioselective metal-catalyzed allylic alkylation of activated nitronates (α -nitroesters) the reader is referred to the following studies and references cited therein: (a) Ohmatsu, K.; Ito, M.; Kunieda, T.; Ooi, T. Ion-Paired Chiral Ligands for Asymmetric Palladium Catalysis. *Nat. Chem.* **2012**, *4*, 473–477. (b) Trost, B. M.; Schultz, J. E.; Bai, Y. Development of Chemo- and Enantioselective Palladium-Catalyzed Decarboxylative Asymmetric Allylic Alkylation of α -Nitroesters. *Angew. Chem., Int. Ed.* **2019**, *58*, 11820–11825. (c) Davison, R. T.; Parker, P. D.; Hou, X.; Chung, C. P.; Augustine, S. A.; Dong, V. M. Enantioselective Coupling of Nitroesters and Alkynes. *Angew. Chem., Int. Ed.* **2021**, *60*, 4599–4603.

(13) For a recent review on alcohol-mediated carbonyl allylation, see: Kim, S. W.; Zhang, W.; Krische, M. J. Catalytic Enantioselective Carbonyl Allylation and Propargylation via Alcohol-Mediated Hydrogen Transfer: Merging the Chemistry of Grignard and Sabatier. *Acc. Chem. Res.* **2017**, *50*, 2371–2380.

(14) (a) Meza, A. T.; Wurm, T.; Smith, L.; Kim, S. W.; Zbieg, J. R.; Stivala, C. E.; Krische, M. J. Amphilic π -Allyliridium *C,O*-Benzooate Enable Regio- and Enantioselective Amination of Branched Allylic Acetates Bearing Linear Alkyl Groups. *J. Am. Chem. Soc.* **2018**, *140*, 1275–1279. (b) Kim, S. W.; Schwartz, L. A.; Zbieg, J. R.; Stivala, C. E.; Krische, M. J. Regio- and Enantioselective Iridium-Catalyzed Amination of Racemic Branched Alkyl-Substituted Allylic Acetates with Primary and Secondary Aromatic and Heteroaromatic Amines. *J. Am. Chem. Soc.* **2019**, *141*, 671–676. (c) Kim, S. W.; Schempp, T. T.; Zbieg, J. R.; Stivala, C. E.; Krische, M. J. Regio- and Enantioselective Iridium-Catalyzed *N*-Allylation of Indoles and Related Azoles with Racemic Branched Alkyl-Substituted Allylic Acetates. *Angew. Chem., Int. Ed.* **2019**, *58*, 7762–7766.

(15) DFT calculations were performed at the M06/6-311+G(d,p)-SDD(Ir)/SMD(NMP)//B3LYP-D3/6-31G(d)-SDD(Ir)/SMD(NMP) level of theory. See the Supporting Information for computational details.

(16) For recent computational studies of Ir-catalyzed allylation reactions, see: (a) Liu, W.-B.; Zheng, C.; Zhuo, C.-X.; Dai, L.-X.; You, S.-L. Iridium-Catalyzed Allylic Alkylation Reaction with *N*-Aryl Phosphoramidite Ligands: Scope and Mechanistic Studies. *J. Am. Chem. Soc.* **2012**, *134*, 4812–4821. (b) Bhaskararao, B.; Sunoj, R. B. Origin of Stereodivergence in Cooperative Asymmetric Catalysis with Simultaneous Involvement of Two Chiral Catalysts. *J. Am. Chem. Soc.* **2015**, *137*, 15712–15722. (c) Madrahimov, S. T.; Li, Q.; Sharma, A.; Hartwig, J. F. Origins of Regioselectivity in Iridium Catalyzed Allylic Substitution. *J. Am. Chem. Soc.* **2015**, *137*, 14968–14981. (d) Butcher, T. W.; Hartwig, J. F. Enantioselective Synthesis of Tertiary Allylic Fluorides by Iridium-Catalyzed Allylic Fluoroalkylation. *Angew. Chem., Int. Ed.* **2018**, *57*, 13125–13129. (e) Sorlin, A. M.; Mixdorf, J. C.; Rotella, M. E.; Martin, R. T.; Gutierrez, O.; Nguyen, H. M. The Role of Trichloroacetimidate To Enable Iridium-Catalyzed Regio- and Enantioselective Allylic Fluorination: A Combined Experimental and Computational Study. *J. Am. Chem. Soc.* **2019**, *141*, 14843–14852.

(17) Kim, S. W.; Meyer, C. C.; Mai, B. K.; Liu, P.; Krische, M. J. Inversion of Enantioselectivity in Alene Gas vs Allyl Acetate Reductive Aldehyde Allylation Mediated by 2-Propanol Guided by Metal-Centered Stereogenicity: An Experimental and Computational Study. *ACS Catal.* **2019**, *9*, 9158–9163.

(18) Here, the computed charges on the hydrogen atoms were summed into the carbon atoms. The NPA charges of the carbon atoms alone reveal the same electrophilicity trends. See the Supporting Information for details.

(19) Ward, T. R. Regioselectivity of Nucleophilic Attack on [Pd(allyl)(phosphine)(imine)] Complexes: A Theoretical Study. *Organometallics* **1996**, *15*, 2836–2838.

(20) When the C3 of crotyl is *trans* to the carbon of the *C,O*-benzoate ligand, the η^1 coordination of crotyl is more favorable than the η^3 coordination. These complexes with long Ir–C3 distances are highlighted using red circles in Figure 4B.

(21) Coe, B. J.; Glenwright, S. J. Trans-effects in Octahedral Transition Metal Complexes. *Coord. Chem. Rev.* **2000**, *203*, 5–80.

(22) Mata, Y.; Pàmies, O.; Diéguez, M. Pyranoside Phosphite-Oxazoline Ligand Library: Highly Efficient Modular P,N Ligands for Palladium-Catalyzed Allylic Substitution Reactions. A Study of the Key Palladium Allyl Intermediates. *Adv. Synth. Catal.* **2009**, *351*, 3217–3234.

(23) The π -allyliridium *C,O*-benzoate catalyst developed in our laboratory was recently used to catalyze asymmetric allylic alkylations of malonates: Zhang, T.-Y.; Deng, Y.; Wei, K.; Yang, Y.-R. Enantioselective Iridium-Catalyzed Allylic Alkylation of Racemic Branched Alkyl-Substituted Allylic Acetates with Malonates. *Org. Lett.* **2021**, *23*, 1086–1089.